

Ab initio calculations of the thermodynamics and phase diagram of zirconiumYan-Jun Hao,^{1,2,*} Lin Zhang,^{1,†} Xiang-Rong Chen,² Ling-Cang Cai,¹ Qiang Wu,¹ and Dario Alfè³¹Laboratory for Shock Wave and Detonation Physics Research, Institute of Fluid Physics, Chinese Academy of Engineering Physics, P.O. Box 919-102, Mianyang 621900, People's Republic of China²College of Physical Science and Technology, Sichuan University, Chengdu 610064, People's Republic of China³Department of Earth Sciences, University College London, Gower Street, London WC1E 6BT, United Kingdom

(Received 5 May 2008; revised manuscript received 13 July 2008; published 1 October 2008)

The finite-temperature density-functional theory and quasiharmonic lattice dynamics are used to calculate the Gibbs free energy and quasiharmonic phonons of the hexagonal-close-packed (hcp) and omega (ω) crystal structures for Zr. The hcp phonon dispersions agree with experiment; the ω phonon dispersions have not been measured yet. From the free energy, the volume thermal expansion coefficients of α -Zr are predicted. The calculated volume thermal expansion coefficients for α -Zr are in good agreement with the experiment data at $T > 100$ K. Our calculated results found that at zero-temperature the lowest-energy phase is not the ω but the hcp phase. This conclusion is in accordance with the result of Schnell and Albers, but in disagreement with those of Ahuja *et al.* and Jona and Marcus. The predicted phase boundary of $\alpha \rightarrow \omega$ is in good agreement with the available experiment; however, other theoretical results are far from the experiment at high temperatures.

DOI: [10.1103/PhysRevB.78.134101](https://doi.org/10.1103/PhysRevB.78.134101)

PACS number(s): 64.70.K-

As one of the group IV transition metals, zirconium has been broadly applied in aerospace, medical, and nuclear fields due to their high strength, light weight, corrosion resistance, and so on.¹ In addition, Zr has a narrow d band in the midst of a broad sp band, which has an impact on its electronic and superconducting properties. The electronic transfer between the broad sp band and the narrow d band is the driving force behind many structural and electronic transitions in group IV transition metal materials.²

The thermodynamic properties of zirconium have been the subject of many experimental and theoretical studies. Experimentally, at ambient conditions, Zr is a hexagonal-close-packed (hcp) structure (the α phase).³ It transforms martensitically into the body-centered-cubic (bcc) structure (the β phase) at temperatures higher than 1136 K. When the pressure is increased at room temperature, a martensitic phase transformation into the omega structure (ω phase, AlB₂ type) is observed between 2 and 7 GPa.³⁻⁸ However, it is now believed to occur at ca. 2.0 GPa at room temperature.^{7,8} At even higher pressures, 30–35 GPa, Zr exhibits a martensitic transformation into the bcc structure.⁹⁻¹¹

Theoretically, Ahuja *et al.*¹² and Jona and Marcus¹³ predicted that at $p=0$, the lowest-energy phase is the ω phase by using Hedin-Lundqvist parametrization for exchange and correlation potential within the local-density approximation without any geometry optimization and the full-potential linearized augmented plane-wave method within the local-density approximation, respectively. Ostanin and Trubitsin¹⁴ reported the phase diagram of $\alpha \rightarrow \omega$ and found that phase transition $\alpha \rightarrow \omega$ is 5.4 GPa at 300 K by the full-potential linear muffin-tin orbital (FP-LMTO) method incorporating information from experimental data. In another theoretical work by Schnell and Albers¹⁵, the phase diagram of zirconium is constructed using tight-binding (TB) methods. They found that the hcp phase is the most stable zero-temperature phase for Zr if zero-point motion effects are added to the enthalpy, and this conclusion is inconsistent with previous theoretical calculations.^{12,13} Moreover, the phase boundaries of $\alpha \rightarrow \omega$ calculated by Ostanin and Trubitsin¹⁴ and Schnell

and Albers¹⁵ are in disagreement from the experiment results at high temperatures.

Up to now, Zr is still controversial in high-pressure structural phase transitions especially at higher temperatures. Therefore, we used here the finite temperature density-functional theory and quasiharmonic lattice dynamics to calculate the phase boundary of $\alpha \rightarrow \omega$ and phonon dispersions. The calculated phonon dispersions for α -Zr are in accordance with the experimental measurements. The volume thermal expansion coefficients for α -Zr are predicted and the results agree well with the experiment data at $T > 100$ K. It is found that the zero-temperature ground state is the hcp structure and this result is in accord with the result of Schnell and Albers¹⁵, but in disagreement with others.^{12,13} The predicted $\alpha \rightarrow \omega$ phase boundary is in better agreement with the experiment than the other theoretical calculations.

Free energy calculations were performed in the framework of the frozen core all-electron projector augmented wave (PAW)^{16,17} method as implemented in the Vienna *ab initio* simulation package (VASP).¹⁸ The plane wave energy cutoff was set to 500 eV. Exchange and correlation potentials were treated within the generalized gradient approximation of Perdew, Burke, and Ernzerhof (PBE).¹⁹ In the PAW method, the effect of core electrons and nuclei is replaced by an effective ionic potential and only the valence electrons, which are directly involved in chemical bonding, are considered. The valence electrons for zirconium are in the $4s^2 4p^6 4d^2 5s^2$ configuration. The integration over the Brillouin zone (BZ) was performed on a grid of special k points determined according to the Monkhorst-Pack scheme.²⁰ Relaxation procedures at zero T were carried out according to the Methfessel-Paxton scheme,²¹ while accurate total energy calculations were performed by means of the linear tetrahedron method with Blöchl's correction.²² The finite temperature for electric structure and force calculations were implemented within the Fermi-Dirac-smearing approach.²³ All necessary convergence tests were performed and the self-consistency convergence of the electronic free energy of all phase considered was set to 10^{-6} eV/cell. The convergence

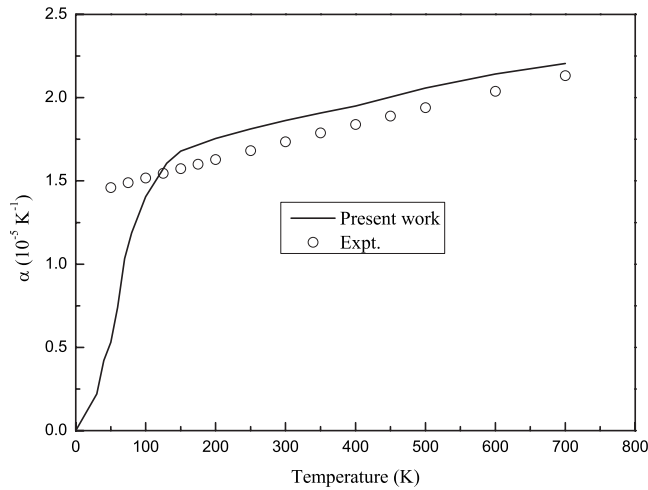


FIG. 1. The volume thermal expansion coefficients of α -Zr. The open symbols are taken from Goldak *et al.* (Ref. 28).

of the vibrational free energies of the hcp and omega structures with respect to the k point grid and the energy cutoff was attained. The phonon frequency calculations were carried out in the framework of the supercell approach using the small displacement method described in Refs. 24–26. To obtain a vibrational free energy converged within 1 meV, we used $3 \times 3 \times 3$ supercells for α -Zr and $3 \times 3 \times 2$ for ω -Zr, respectively. Forces induced by small atomic displacements were calculated using the VASP program. The phonon dispersion calculations were performed at a number of electronic temperatures up to 900 K. It was found that the phonon dispersions were insensitive to the electronic temperature and, consequently, further calculations were performed at an electronic temperature of 300 K. The free energy was calculated as the sum of the electronic and vibrational contributions. The equation of state was obtained by accurate numerical interpolation of the calculated Helmholtz free energies using the Vinet equation of state (EOS).²⁷

We calculate the total free energy at a number of different temperatures, for each temperature fitted the total free energy to the Vinet EOS.²⁷ The volume thermal expansion coefficients of α -Zr are obtained. In Fig. 1, we show the calculated volume thermal expansion coefficients for α -Zr together with experimental data.²⁸ Here, excellent agreement is found between the calculated and experimental coefficients of volume thermal expansion at $T > 100$ K. However, the experimental data display some peculiar features, i.e., the thermal expansion coefficients show only a slight variation with increasing temperature. Furthermore, if one extrapolated the experimental data along its tangent from 50 to 0 K, it would be positive and considerably different from zero. A general property of all materials is that the thermal expansion coefficients should approach zero at $T=0$ K. These suggest that the experimental thermal expansion data of Zr are indeed somewhat questionable.

Figure 2 compares our calculated phonon dispersions for the α structure to experimental data.²⁹ The α phonons are consistent with the experimental values for the high-energy optical and acoustic branches; these are important for modeling the shuffle during martensitic transformation. The cal-

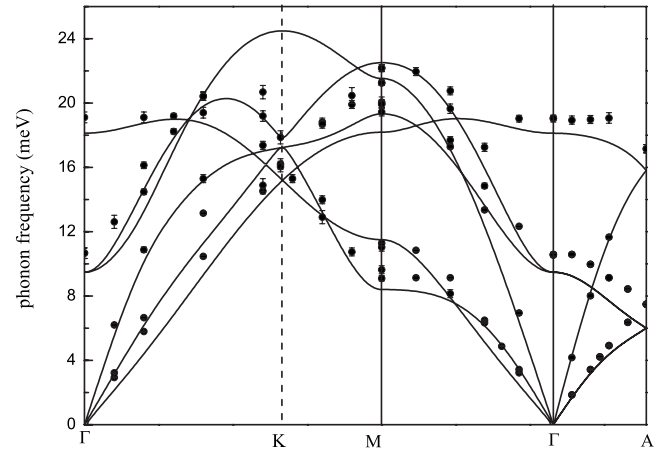


FIG. 2. Comparison of the calculated phonon dispersions for α -Zr with experimental phonon data. The solid line is the present calculation at room temperature ($T=300$ K) equilibrium volume. The solid squares with error bars represent the experimental data from inelastic neutron scattering data at $T=295$ K (Ref. 29).

culated phonon dispersions for ω -Zr are predicted in Fig. 3. It is noted that the ω phonons are expectedly stiffer along the c axis than in the basal plane due to the low c/a ratio. Unfortunately, there are not yet experimental data on phonon dispersions of ω -Zr to compare with our calculated results.

Figure 4 represents the calculated E - V and G - P data. It is noted that the α phase is more stable than the ω phase at 0 K. This conclusion is also supported by the calculated result of Schnell and Albers¹⁵ and is in disagreement with the other calculations.^{12,13} To predict the phase boundary of $\alpha \rightarrow \omega$, we calculate here the Gibbs free energy of the hexagonal-close-packed (hcp, α) and omega (ω) crystal structures. The Gibbs energy difference between the hcp and omega structures (ΔG) of Zr as a function of pressure for several temperatures is reported in Fig. 5. At 0 K, ΔG is already negative at low pressures and, consequently, the hcp structure appears in the calculated phase diagram. The phase transition of $\alpha \rightarrow \omega$ oc-

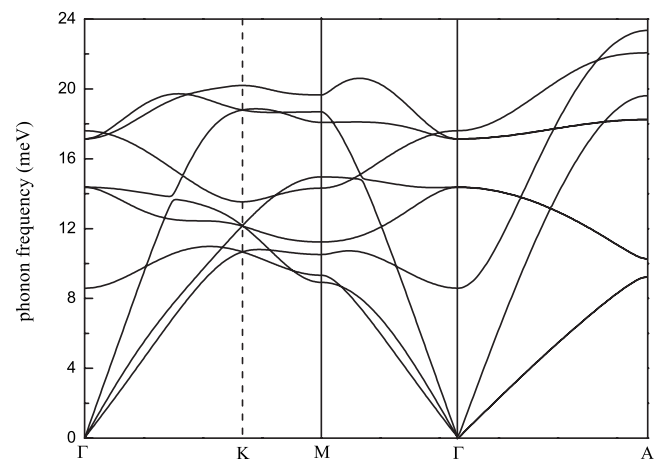


FIG. 3. Predicted phonon dispersions in the ω crystal structure at room-temperature ($T=300$ K) equilibrium volume. As expected from the c/a ratio of 0.623, the phonon modes are stiffer along the [001] direction than the basal plane directions [100] and [010].

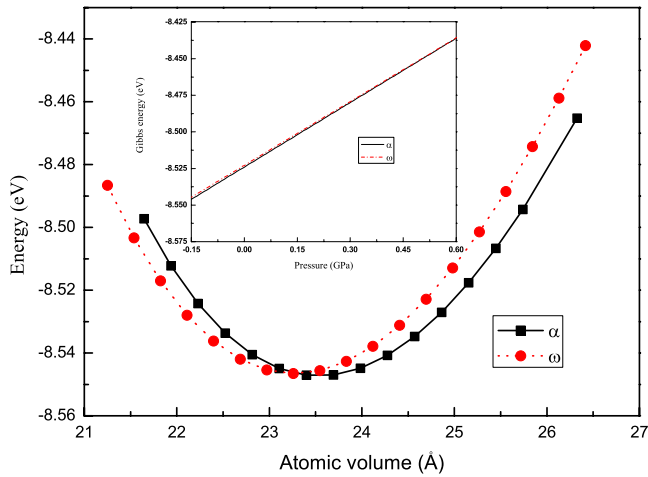


FIG. 4. (Color online) The energy as a function of atomic volume at $T=0$ K. In the inset, the Gibbs free energy as a function of pressure is presented.

transitions occur at ca. 1.7 GPa at $T=300$ K, which agrees well with what had generally been believed.^{7,8} At the same time, under compression ΔG increases and eventually becomes positive, indicating a stabilization of the ω structure and at higher temperatures the pressure of the $\alpha \rightarrow \omega$ transition increases even further.

The pressure-volume isotherms of the Zr at $T=300$ K are compared with previous results in Fig. 6. The solid curve is the present EOS. The squares are taken from Zhao *et al.*³⁰ The triangles are experimental results from Liu *et al.*³¹ The open symbols are experimental data from Akahama *et al.*¹¹ The dotted curve gives the Birch-Murnaghan fit of Xia *et al.*⁹ for the ω phase. The present EOS agrees very well with the experimental data of Akahama *et al.*¹¹ Our atomic volumes at high pressure are slightly higher than those obtained by other experiments.^{9,30,31} This might be due to the systematic errors existing among different experimental techniques as discussed by Zhao *et al.*³⁰

Once the free energies of the α phase and ω structure are

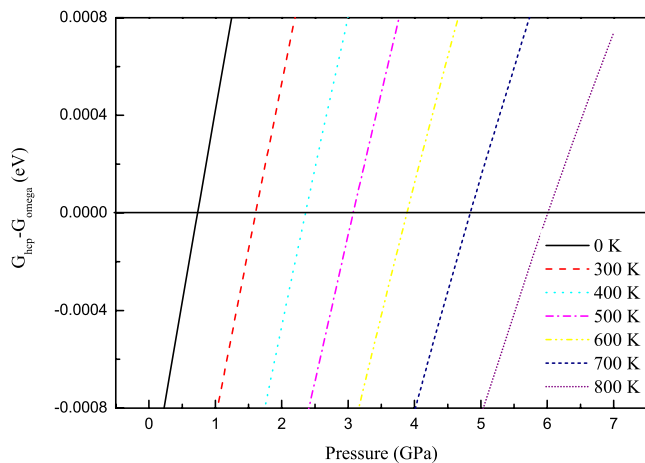


FIG. 5. (Color online) The difference of the Gibbs free energies of the hcp and omega phases of Zr as a function of pressure for several temperatures. A positive difference indicates that the ω phase is more stable.

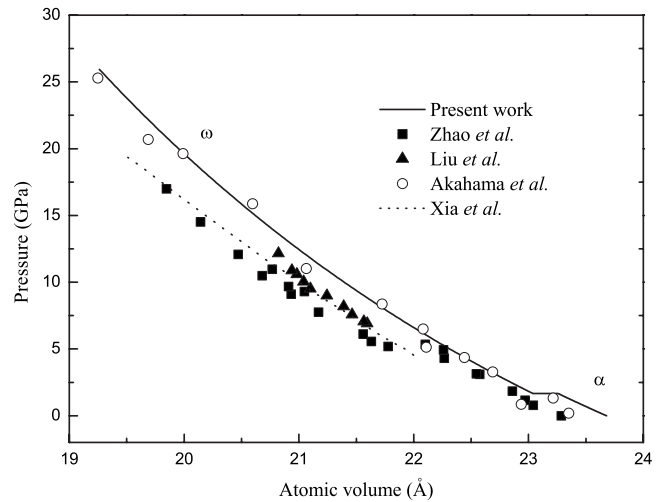


FIG. 6. Pressure as a function of atomic volume of Zr at $T=300$ K. The solid line is the present work. The squares are taken from Zhao *et al.* (Ref. 30). The triangles are experimental results from Liu *et al.* (Ref. 31). The open symbols are experimental data from Akahama *et al.* (Ref. 11). The dotted curve gives the Birch-Murnaghan fit of Xia *et al.* (Ref. 9) for the ω phase.

determined, the phase boundary can be obtained by equating Gibbs free energies at a given pressure and temperature. The phase diagram of Zr is predicted in Fig. 7, compared with other theoretical calculations^{14,15} and experiment.⁷ The dotted line is from calculations of Ostanin and Trubitsin,¹⁴ who obtained the phase diagram by the FP-LMTO method with experimental parameter input. It is observed that although the shape of their transition line is similar to the present calculation, the transition pressures computed by Ostanin and Trubitsin are higher at high temperatures. The dashed-dotted curve is TB results of Schnell and Albers¹⁵. It is seen that their transition pressures are higher than ours at T

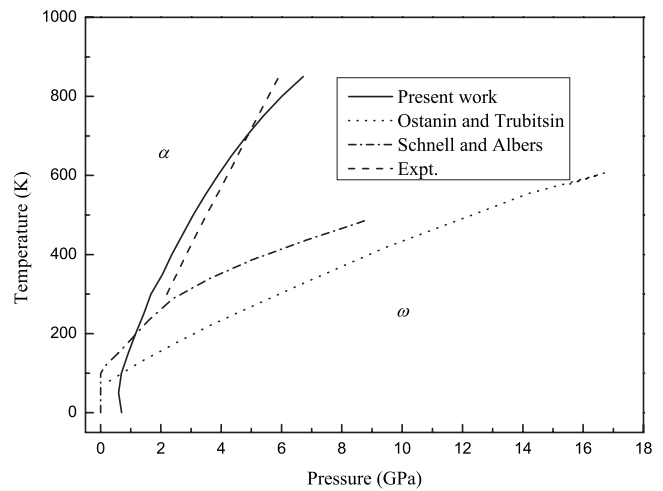


FIG. 7. Comparison of phase diagram of Zr from present calculations with previous experiment and other theoretical results. The solid line is present work. The dotted line is taken from Ostanin and Trubitsin (Ref. 14). The dashed-dotted line is result of tight binding of Schnell and Albers (Ref. 15). The dashed line represents experimental data point given by Young (Ref. 7).

>200 K. At temperatures lower than this, the phase transition pressure of Schnell and Albers decreases slowly. The dashed line represents experimental data point given by Young.⁷ It is seen that the present phase boundary is in excellent agreement with the available experiment;⁷ however, other theoretical results^{14,15} are far from the experimental result at high temperatures.

In summary, we have calculated the phase diagram of $\alpha \rightarrow \omega$ of Zr by using the finite temperature density-functional theory and quasiharmonic lattice dynamics. Our work is based on the calculation of the Gibbs free energy of α and ω phases, and for each fixed temperature the phase transition pressure is determined by the point at which the two free energies cross. Our calculated phase boundary is in better agreement with the available experimental data than other theoretical results. Our calculated results found that the α

structure is most stable at zero temperature and this conclusion agrees well with that of Schnell and Albers. For the ω structure the phonon dispersions are predicted. The calculated volume thermal expansion coefficients for α -Zr are also predicted and the results are in good agreement with the experimental data at $T > 100$ K.

We acknowledge the support for this work by the National Key Laboratory Fund for Shock Wave and Detonation Physics Research of the China Academy of Engineering Physics under Grant No. 9140C6702030802, the National Natural Science Foundation of China under Grants No. 10776029/A06 and No. 10576020, and the NSAF under Grant No. 10776022. We also acknowledge the support by Rui-Feng Co.

*Author to whom correspondence should be addressed. FAX: +86-816-2485139; yjhao@126.com.

†Author to whom correspondence should be addressed. zhanglinbox@263.net

¹Y. K. Vohra and P. T. Spencer, Phys. Rev. Lett. **86**, 3068 (2001).

²A. L. Kutepov and S. G. Kutepova, Phys. Rev. B **67**, 132102 (2003).

³S. K. Sikka, Y. K. Vohra, and R. Chidambaram, Prog. Mater. Sci. **27**, 245 (1982).

⁴Y. K. Vohra, J. Nucl. Mater. **75**, 288 (1978).

⁵J. C. Jamieson, Science **140**, 72 (1963).

⁶B. Olinger and J. C. Jamieson, High Temp. - High Press. **5**, 123 (1973).

⁷D. A. Young, *Phase Diagrams of the Elements* (University of California, Berkeley, 1991).

⁸V. A. Zilbershteyn, N. P. Chistotina, A. A. Zharov, N. S. Grishina, and E. I. Estrin, Fiz. Met. Metalloved. **39**, 445 (1975).

⁹H. Xia, S. J. Duclos, A. L. Ruoff, and Y. K. Vohra, Phys. Rev. Lett. **64**, 204 (1990).

¹⁰H. Xia, A. L. Ruoff, and Y. K. Vohra, Phys. Rev. B **44**, 10374 (1991).

¹¹Y. Akahama, M. Kobayashi, and H. Kawamura, J. Phys. Soc. Jpn. **60**, 3211 (1991).

¹²R. Ahuja, J. M. Wills, B. Johansson, and O. Eriksson, Phys. Rev. B **48**, 16269 (1993).

¹³F. Jona and P. M. Marcus, J. Phys.: Condens. Matter **15**, 5009 (2003).

¹⁴S. A. Ostanin and V. Y. Trubitsin, Phys. Rev. B **57**, 13485 (1998).

¹⁵I. Schnell and R. C. Albers, J. Phys.: Condens. Matter **18**, 1483 (2006).

¹⁶P. E. Blöchl, Phys. Rev. B **50**, 17953 (1994).

¹⁷G. Kresse and D. Joubert, Phys. Rev. B **59**, 1758 (1999).

¹⁸G. Kresse and J. Furthmüller, Phys. Rev. B **54**, 11169 (1996).

¹⁹J. P. Perdew, K. Burke, and M. Ernzerhof, Phys. Rev. Lett. **77**, 3865 (1996).

²⁰H. J. Monkhorst and J. D. Pack, Phys. Rev. B **13**, 5188 (1976).

²¹M. Methfessel and A. T. Paxton, Phys. Rev. B **40**, 3616 (1989).

²²P. E. Blöchl, O. Jepsen, and O. K. Andersen, Phys. Rev. B **49**, 16223 (1994).

²³N. D. Mermin, Phys. Rev. **137**, A1441 (1965).

²⁴D. Alfè, program available from <http://chianti.geol.ucl.ac.uk/~dario>

²⁵D. Alfè, G. D. Price, and M. J. Gillan, Phys. Rev. B **64**, 045123 (2001).

²⁶G. Kresse, H. Furthmüller, and J. Hafner, Europhys. Lett. **32**, 729 (1995).

²⁷P. Vinet, J. R. Smith, J. Ferrante, and J. H. Rose, Phys. Rev. B **35**, 1945 (1987).

²⁸J. Goldak, L. T. Lloyd, and C. S. Barrett, Phys. Rev. **144**, 478 (1966).

²⁹C. Stassis, J. Zarestky, D. Arch, O. D. McMasters, and B. N. Harmon, Phys. Rev. B **18**, 2632 (1978).

³⁰Y. S. Zhao, J. Z. Zhang, C. Pantea, J. Qian, L. L. Daemen, P. A. Rigg, R. S. Hixson, G. T. Gray III, Y. P. Yang, L. P. Wang, Y. B. Wang, and T. Y. Uchida, Phys. Rev. B **71**, 184119 (2005).

³¹W. Liu, B. S. Li, L. P. Wang, J. Z. Zhang, and Y. S. Zhao, Phys. Rev. B **76**, 144107 (2007).